PIOTR MAŁKOWSKI*[#], ŁUKASZ OSTROWSKI*

CONVERGENCE MONITORING AS A BASIS FOR NUMERICAL ANALYSIS OF CHANGES OF ROCK-MASS QUALITY AND HOEK-BROWN FAILURE CRITERION PARAMETERS DUE TO LONGWALL EXCAVATION

POMIARY KONWERGENCJI JAKO PODSTAWA ANALIZY NUMERYCZNEJ ZMIAN JAKOŚCI GÓROTWORU I PARAMETRÓW KRYTERIUM WYTRZYMAŁOŚCIOWEGO HOEKA-BROWNA WYNIKAJĄCYCH Z EKSPLOATACJI ŚCIANOWEJ

In the longwall exploitation system, the main gates are subject of the most intensive movements of the rock mass, where the proximity of the excavation front is a key factor. The paper presents the results of a research on the constants mb and s of Hoek-Brown failure criterion for the rocks surrounding the gallery: shale, sandy shale, coal and medium-grained sandstone, in relation to the distance to longwall face. The research comprised numerical modeling based on convergence monitoring records. The convergence measurements were carried out on three stations in a selected maingate in a coal mine from Upper Silesia Coal Basin near Jastrzębie-Zdrój, concurrently with changing distance to the longwall face. The measured were the width, the height and the heave of the floor of the gate. The measurements showed that the convergence at the longwall-maingate crossing was 1.5-3 times greater than in the locations much further from the longwall face. It was demonstrated that this effect was due to continuously changing properties of the rock-mass surrounding the gallery that can be expressed as decreasing empirical parameters mb i s of Hoek-Brown's criterion. These parameters are decreasing exponentially together with the distance to the longwall face The consistency between the theoretical and factual curve varies between 70% to 98%. The change of each of the parameters can be described by general equation $P = a \cdot \exp(-b \cdot d)$, where a, b are constants, and d is the distance to the excavation face. The authors highlight that during the measurements period the horizontal stress was 1.45 to 1.61 times greater than the concurrent vertical stress. The so high horizontal stress causes heave of unsupported gallery floor which is commonly observed in the mines in Silesia.

Keywords: Hoek-Brown failure criterion, back analysis, convergence of mining gallery, longwall excavation, m and s parameters

Chodniki przyścianowe w systemie eksploatacji ścianowej są najbardziej narażone na intensywne przemieszczenia skał. Wraz ze zmianą położenia frontu eksploatacji skały przechodzą wolno w stan

* AGH UNIVERSITY OF SCIENCE AND TECHNOLOGY, GEOMECHANICS, CIVIL ENGINEERING AND GEOTECHNICS, AL. MICKIEWICZA 30, 30-059, KRAKÓW, POLAND

[#] Corresponding author: malkgeom@agh.edu.pl

zniszczenia, coraz bardziej przemieszczając się do środka wyłomu. Aby można było skutecznie prze-widywać konwergencję wyrobisk przyściennych należy właściwie określić właściwości skał w fazie pozniszczeniowej. Wybierając warunek wytrzymałościowy Hoeka-Browna – stałe *mb* i *s*, zależne od wskaźnika jakości górotworu RMR lub wskaźnika GSI.

W artykule wyznaczono spadek parametrów pozniszczeniowych skał budujących górotwór w rejonie omawianego wyrobiska – łupków ilastych, łupków piaszczystych, węgli i piaskowców średnioziarnistych – w zależności od odległości od frontu ściany. W tym celu wykonano symulacje numeryczne, wykorzystując wyniki pomiarów konwergencji. Pomiary konwergencji wykonano w wyrobisku przyściennym jednej z kopalń węgla GZW w rejonie Jastrzębia na trzech bazach pomiarowych wraz ze zmieniającą się odległością baz pomiarowych od czoła ściany. Badania obejmowały wyznaczenie szerokości, wysokości i wypiętrzenia spągu chodnika. Pomiary wykazały, że konwergencja na skrzyżowaniu ściana – chodnik osiąga wartość 1,5-3-krotnie większą, niż dla przypadku, gdy front eksploatacji znajduje się w znacznej odległości od baz pomiarowych. Stwierdzono, że przyczyną takiego stanu rzeczy jest stale zmieniająca się jakość górotworu, która skutkuje obniżeniem parametrów empirycznych warunku wytrzymałościowego Hoek'a-Browna *mb* i *s* skał występujących w otoczeniu wyrobiska. Parametry te maleją eksponencjalnie wraz ze zbliżaniem się frontu ściany, a zgodność pomiędzy krzywą rzeczywistą a teoretyczną dla występujących przemieszczeń wyrobiska waha się od 70% do 98%. Zmianę dowolnego z powyższych parametrów *P* można opisać funkcją o ogólnym równaniu: $P = a \cdot \exp(-b \cdot d)$, gdzie *a* i *b* to stałe, a *d* to odległość od frontu ściany.

Na uwagę zasługuje również analiza naprężeń poziomych w górotworze, jakie musiały wystąpić podczas prowadzenia pomiarów, które są 1,45-1,61 razy większe od występujących wówczas naprężeń pionowych. Tak duże naprężenia poziome mają istotny wpływ na wartości wypiętrzania nieobudowanego spągu, co znajduje potwierdzenie podczas prowadzenia prac górniczych w kopalniach JSW.

Słowa kluczowe: konwergencja wyrobiska, eksploatacja ścianowa, kryterium wytrzymałościowe Hoeka--Browna, parametry *m* i *s*, analiza odwrotna

1. Introduction

Longwall with roof fall is the prevailing system of coal exploitation in Poland hence the coal production depends largely on the stability and uninterrupted functioning of the gateroads. Together with the exploitation reaching deeper coal beds and related growing of geological and mining difficulties, the prevention of the main gates from collapse or deformation becomes the major challenge for the engineers and the designers to ensure cost-effective production and safety of the crew.

Among various types of mining galleries, the most intense deformation of the rock-mass, such as roof caving, heaving of the floor, or converging of the sidewalls is observed in the gateroads. These deformations depend on many mining and geological factors identified by experts (Bieniawski, 1987; Brady & Brown, 2006; Chudek & Duży, 2002; Lubosik & Walentek, 2016; Majcherczyk & Małkowski, 2003; Peng, 2006; Prusek 2008; 2015; Małkowski et al., 2016a; Mohammadi et al., 2018): strength parameters, excavation history (e.g. goaves and boundaries of mining fields), presence of pillars and abandoned deposits, geological features like faults or presence of weak rocks, groundwater condition, dynamic phenomena (rockbursts), and the type and construction details of the support. The authors indicate that in the case of gateroads the main factor affecting the convergence is the excavation front – its advance rate and length. They all point out (Bieniawski, 1987; Junker & Achilles, 2006; Majcherczyk & Małkowski, 2003; Peng, 2006; Prusek, 2008; Niedbalski et al., 2013) that the highest stress in the bed excavated with the caving method may reach a value six times the initial stress related to the depth of the coal bed. It has to be noted that the highest stress develops not at the exact longwall face but at distance *L* from it (Fig. 1), due to formation of fractures. Apparently, the destruction of the rock mass starts ahead of the longwall face and intensifies with the decreasing distance to the face.

Therefore, for the analysis of the stability of the gate, the three key questions need to be answered:

1. In what distance from the longwall face its impact on the rock mass becomes significant?
2. How big are the vertical and horizontal stress that cause the deformation and fracturing of the rock mass in its vicinity?
3. What is the degree of rock mass deterioration and what is the change of its quality?
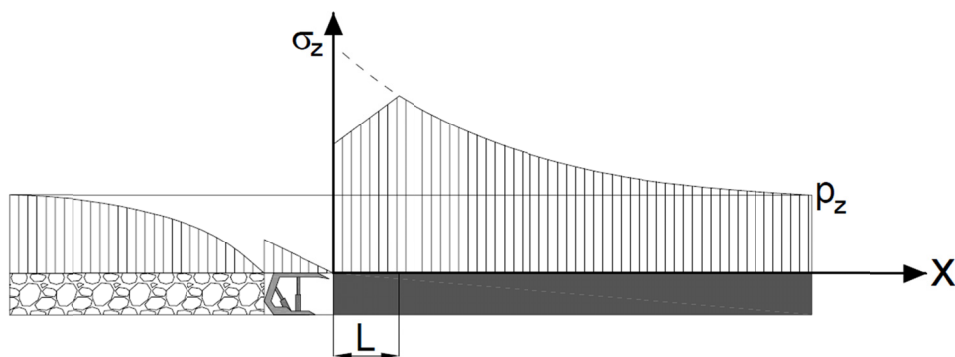

Fig. 1. Distribution of stress ahead and behind the longwall face

Once the change of the rock parameters is determined it would be feasible to develop geo-mechanical model utilizing failure criterion (either Coulomb-Mohr or Hoek's-Brown), and further forecast with a good confidence the destruction zones and the deformations.

This paper presents the results of the numerical analysis based on convergence measurements carried out in the gateroad D-2 in Zofiówka mine in Upper Silesia Coal Basin (USCB). The back analysis allowed for determination of the change of the empirical rock mass quality parameters m_b and s of the Hoek-Brown failure criterion, for the carboniferous rocks. The alteration of these parameters was evaluated for shale, sandy shale, coal and medium grained sandstones. By back analysis there were also determined the magnitudes of the horizontal stress that developed in the gallery surround and could produce the recorded values of convergence.

2. The change of rock mass properties around the longwall excavation, and deformation of the gates in the stress condition

2.1. Stress condition around the opening

The modern technologies allow for *in situ* stress measurements around the mining workings. Therefore, the analytically obtained values can be verified. The so far carried out measurements (Brown & Hoek, 1978; Han & Zhang, 2010; Nemcik et al., 2006; Staš et al., 2011; Handley, 2013; Butra et al., 2013; Makówka, 2015; Waclawik et al., 2017) confirm the rise of the vertical stress with depth. Whereas, there is no such explicit relationship between the horizontal stress and

depth or vertical stress (Fig. 2-4). The researches from other continents report that the horizontal stress may by higher than the vertical component, which leads to problems with roof and floor stability (Brown & Hoek, 1978; Mark, 1991; Nemcik et al., 2006; Staš et al., 2011; Handley, 2013; Makówka, 2015).
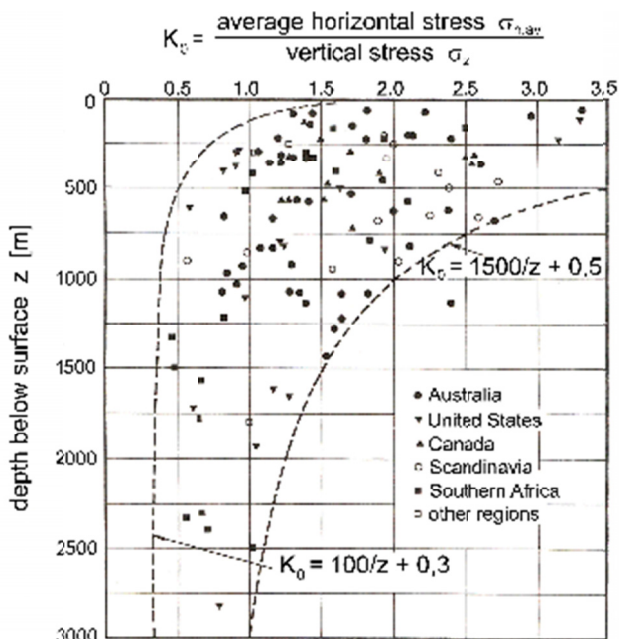

Fig. 2. Value of k_σ coefficient versus depth (Brown & Hoek, 1978)

The k_σ coefficient, defined as a ratio between average horizontal stress $\sigma_{x,y\ sred}$ and vertical stress σ_z, varies with depth and shows the highest values at shallow locations (Fig. 2-4). Only at depths greater than 2500 m the range of its variation becomes smaller and the horizontal stress does not exceed the vertical (Fig. 2). The quoted results show the value of horizontal stress may exceed 3 to 5 times the theoretical vertical stress, and, as highlighted by Nemcik (et al. 2006), significantly increase in fault zones.

It can be read from Fig. 2 that for the average exploitation depth (approx. 800 m) and for the deepest exploitation (approx. 1200 m) in Poland's coal mines, the horizontal stress may be expected up to two times higher than vertical stress. Up today, the few researches carried out in the Upper Silesia Coal Basin in Poland and in Czech Republic show that the stress in one of the horizontal directions is higher than the vertical stress (Staš et al., 2011; Makówka, 2015; Waclawik et al., 2017). In addition, the stress condition starts varying at some distance to the approaching longwall face (Staš et al., 2011; Waclawik et al., 2017), that is linked to fracturing and weakening of the rock. The research shows this distance is in the range from 20 to 160 m and depends on exact position of the stress measurement point, yet the proportion between the maximum and minimum stress remain. Concentration and high value of horizontal stress have the major effect on stability of the gates and are the cause of squeezing.
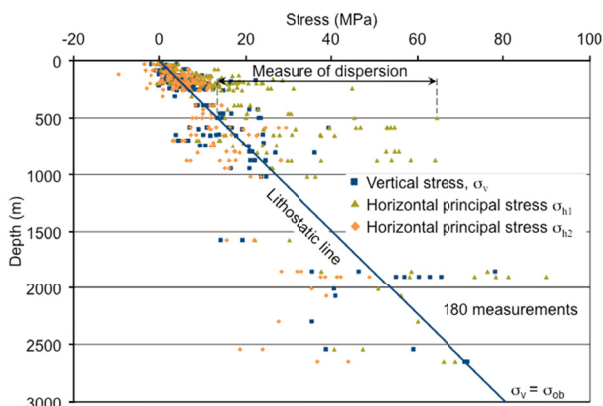
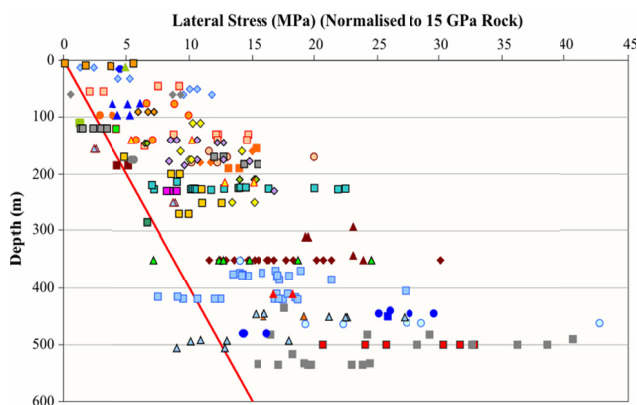Fig. 3. *In-situ* stress measurements in mines in South Africa (Handley, 2013)

Fig. 4. *In-situ* stress measurements in mines in Australia (Nemcik et al., 2006)

2.2. Change of the rock mass quality around the longwall face

In the zones where stress concentrates and exceeds the tension and shear strength the rock breaks. The network of fractures starts developing in the rock mass and is the most intensive at the boundary of collapsing roof (Fig. 5). The changes within the rock structure appear at the distance L from the longwall face as shown in the Fig. 1, where the increase of stress indicates the rock bears the load and remains intact. The decrease of stress signs the progressing failure of the rock.

The quality of the rock mass changes due to development of fractures. Intensity and characteristics of fractures are the major quality factors in the rock mass geotechnical quality classification systems like RMR, GSI, Q, RMI, and others. Subsequently, the mechanical parameters of the rock mass can be inferred from the quality evaluation by these systems, and in case of Hoek's-Brown strength hypothesis (Equation 1), the empirical parameters m_b and s also can be determined (Equations 2 and 3 – Hoek, 2016). It is important notion because this hypothesis is

currently commonly applied to solve geomechanical problems and is often in-built in numerical software. The equations are:

$$\sigma_1 = \sigma_1 + \left(m_b \frac{\sigma_3}{\sigma_c} + s \right)^a \tag{1}$$

$$m_b = m_i \exp\left(\frac{GSI - 100}{28 - 14D} \right) \tag{2}$$

$$s = \exp\left(\frac{GSI - 100}{9 - 3D} \right) \tag{3}$$

where:

σ_c — uniaxial compressive strength, MPa,
D — disturbance factor,
a — the constant which depends upon the rock mass characteristics.

The GSI index can be determined from RMR index using the relationship:
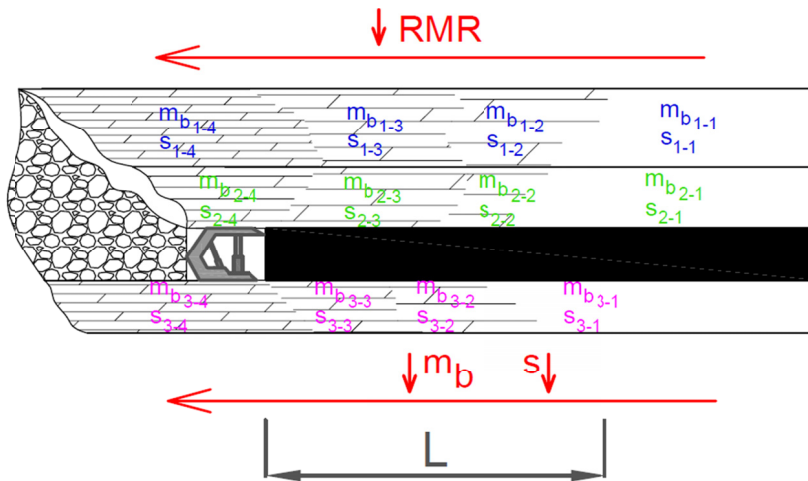
$$GSI = RMR_{89} - 5 \tag{4}$$

Fig. 5. Development of fractures in the rock mass approaching the longwall face

The parameters m_b and s for each rock layer (from 1 to n) continue changing together with the approaching longwall face. It can be described as m_{b1-1} and s_{1-1}, m_{b2-1} and s_{2-1}, and so on for the undisturbed rock mass, and with decreasing values m_{b1-n} and s_{1-n}, m_{b2-n} and s_{2-n} and so on towards the longwall face (Fig. 5).

Obviously, the change of GSI index corresponds with the change of parameters m_b and s of Hoek's-Brown criterion. Both of these parameters will decrease together with decreasing GSI index due to concentration of stress ahead of the exploitation face. Therefore, the assumption of

invariable quality of the rock and constant m_b and s parameters in the exploitation zone is incorrect. Unfortunately, in many cases the numerical models of rock mass in exploitation zones are simplified (Islam et al., 2009; Lian-guo et al., 2009; Basarir et al., 2015). Moreover, as brought up by Singh (2015), there is no evaluation of the changes of rock properties in the analytical solutions of the stability of the openings, and most often the rock mass is considered homogeneous without even differentiating between rock beds. The quantitative results obtained from such simplified assumptions are inadequate.

Faria Santos and Bieniawski jointly stated in 1989 that the key concern for proper solution of geotechnical problems and design of the support is the evaluation of RMR index. Some researchers resolve to apply time related reduction of the mechanical rock parameters to take into account the effect of erosion and propagation of fractures (Yasitli & Unver, 2005; Hosseini et al., 2014). This reduction is empirical. The others introduce in the solutions the so-called expansion factor (Madji et al., 2012) or buckling factor (Sabanimashcool & Li, 2015) that reflect the destruction of rocks induced by the excavation.

The determination of parameters m_b and s requires investigation in triaxial compression condition (Faria Santos & Bieniawski, 1989; Toraño et al., 2002; Hoek, 2016) yet this kind of test on fractured rocks may not be feasible. In these circumstances, the back analysis of measurements of convergence of the gallery becomes the practical solution.

2.3. Deformation of gates

Two stages in the gate functioning time need to be discerned for the analysis of its convergence: first stage when the gate is beyond the excavation impact, and second stage when it is within the impact zone.

In the first stage the gate can be considered as any other gallery, yet having on mind that its life span is much shorter than the main galleries, and its convergence is small until the commencement of longwall excavation (Prusek, 2008; Niedbalski et al., 2013; Małkowski et al., 2016 a,b). Secondary stress and strain conditions form around the opening (concentration of compressional stress within the walls and tensional stress in the roof and floor) under static and deformational load.

In the second stage the approaching longwall face causes intense deformation of the working due to increasing compressional stress in the sidewalls, then increased load on the floor rocks and sometimes additional dynamic loads (Madji & Hassani, 1989; Toraño et al., 2002; Prusek, 2008). The deformation process of the gates is determined largely by the horizontal extent of the abutment zone.

In the conditions of the Upper Silesia Coal Basin the measurable deformations of gateroads related to a longwall excavation appear at 160 m distance from the longwall face, become most intense at 20-80 m distance, and then the rock mass movement stabilizes at 60 to 200 m behind the excavation face (Chudek & Duży, 2002; Majcherczyk & Małkowski, 2003; Niełacny, 2009; Prusek, 2008; Wardas et al., 2013; Herezy, 2013).

The deformation of gateroads in the USCB were subject to many researches and the results are compiled in Table 1. The compilation shows the scale of the problem of maintaining stability of the gateroads, particularly in cases when the main gate is planned to be used twice for two adjacent longwall panels. In some instances, the deformations of the rock mass and support are too big for the reuse of the main gate. The deformations may reach 30-40% of the initial dimensions of the gate, as it is brought up in works by Madji & Hassani (1989) and Toraño (et al. 2002).

Magnitudes of convergence measured in gateroads in Upper Silesian Coal Basin

| Reference	Measured value	Results
Prusek, 2008	Vertical convergence Incl. floor heaving	30÷780 mm 10÷580 mm
	Horizontal convergence	10÷300 mm
Niełacny, 2009	Vertical convergence Incl. floor heaving	100÷870 mm 40÷580 mm
	Horizontal convergence	240÷590 mm
Herezy, 2013	Vertical convergence	80÷900 mm
	Horizontal convergence	50÷400 mm
Wardas et al., 2013	Vertical convergence	670÷810 mm
	Horizontal convergence	320÷840 mm
Niedbalski, Małkowski, Majcherczyk, 2013	Vertical convergence	840÷1260 mm
	Horizontal convergence	300÷710 mm
Prusek, 2015	Vertical convergence	240÷1332 mm
	Horizontal convergence	299÷1871 mm
Lubosik & Walentek, 2016	Vertical convergence Incl. floor heaving	250÷2150 mm 225÷1800 mm
	Horizontal convergence	250÷2100 mm
Wrana & Prusek, 2016	Vertical convergence	80÷1450 mm
	Horizontal convergence	110÷2050 mm
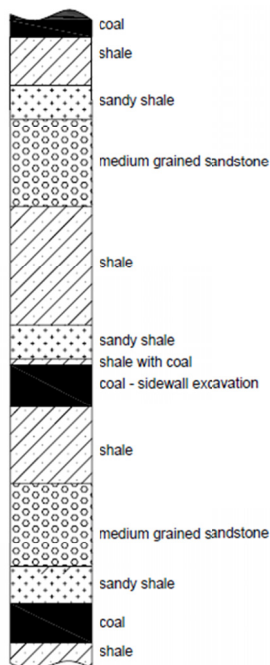
Fig. 6. Geological column at the site

3. Convergence measurements in the maingate D-2

3.1. Mining and geological conditions in the research location

The working subject to the research was within coal bed of a total thickness 4.4. Its floor was 998 to 1030 m deep, and the length of the gate was 1500 m.

The geological column of the rocks above the gate's roof is shown on Fig. 6 and includes (in sequence): shale with laminas of coal, sandy shale, shale with locally sand content, medium grained sandstone, sandy shale and another coal bed (the vertical distance between the coal beds is approx. 28 m).

The samples of rocks exposed directly in the roof, floor and walls were collected and laboratory tested to determine their geomechanical properties. The tests were carried out in accordance with the guidelines by ISRM (Ulusay & Hudson, 2007). The parameters of rocks located further from the contour of the gallery were assumed after

the available technical documentation (Technical documentation, 2016). The values of geomechanical parameters of all rock types around the maingate D-2 are presented in Table 2.

The laboratory results show, for the rock from the immediate roof, the average uniaxial compressive strength 29.9 MPa with the spread of the individual results 18.84÷40.96 MPa. The average elastic modulus of this rock is 5.62 GPa (the range of results 2.96÷7.01 GPa), while Poisson ratio 0.35 (the range of results 0,31÷0,39).

The rock in the floor of the gallery is generally stronger than the rock exposed in the roof, and its parameters derived from laboratory testing are:

- uniaxial compressive strength

$$R_C = 50.3 \text{ MPa } (37.77÷56.05 \text{ MPa}),$$

- Young's modulus

$$E = 4.55 \text{ GPa } (3.01÷6.24 \text{ GPa}),$$

- Poisson ratio

$$v = 0.32 \ (0.16÷0.37).$$

It needs to be pointed out that for each rock type, and for each bed in the roof and floor the values of geomechanical parameters were determined from laboratory testing.

TABLE 2

Geo-mechanical parameters of the rocks in the surround of the maingate D-2

Spot	Rock type	Bed thickness h_i [m]	Unit weight γ_i [kN/m^3]	UCS σ_{ci} [MPa]	Young's modulus E_i [GPa]	Poisson ratio v_i [-]
Roof	Coal	1.0	13.02	10.2	1.57	0.30
	Shale	1.4	25.87	51.7	7.17	0.32
	Sandy shale	3.2	25.32	60.4	10.78	0.28
	Medium grained sandstone	7.8	25.41	58.2	9.52	0.26
	Shale	10.5	25.87	51.7	7.17	0.32
	Sandy shale	3.2	25.01	41.2	6.98	0.32
	Shale	0.6	25.16	29.9	5.62	0.31
Sidewall	Coal	4.4	12.81	12.4	1.86	0.30
Floor	Shale	8.5	24.97	50.3	4.55	0.32
	Medium grained sandstone	5.9	26.97	70.1	6.59	0.28
	Sandy shale	2.8	25.78	58.9	8.87	0.29
	Coal	3.5	12.48	11.9	1.69	0.30
	Shale	9.2	26.73	50.2	6.23	0.29

3.2. Methodology of the research

Convergence measurements were carried out in a period of one and half year in the maingate D-2 in purpose to determine the impact of the exploitation on the gate. The measurements started in April 2015 with one-month frequency and continued during formation of the gallery and later – during its use as a main gate. The results were analyzed in reference to nominal initial

dimensions of the contour: 6.5 m width and 4.225 m height (the working cross-section amounts to 21.58 m^2). The support of the working was steel yielding arch type ŁPCBor 12/4/V34/A at 0.6 m spacing.

Three convergence monitoring stations were installed: at chainage 650KM, 714KM and 735KM. Each station comprised four measurement points MP1, MP2, MP3, MP4 (Fig. 7) that allow for measurement of changes of the contour height H, width W, and heave of the floor u_{fl} (Fig. 7). The floor heave was measured as a change of the distance between the floor and MP1 – MP3 line in 10 locations.
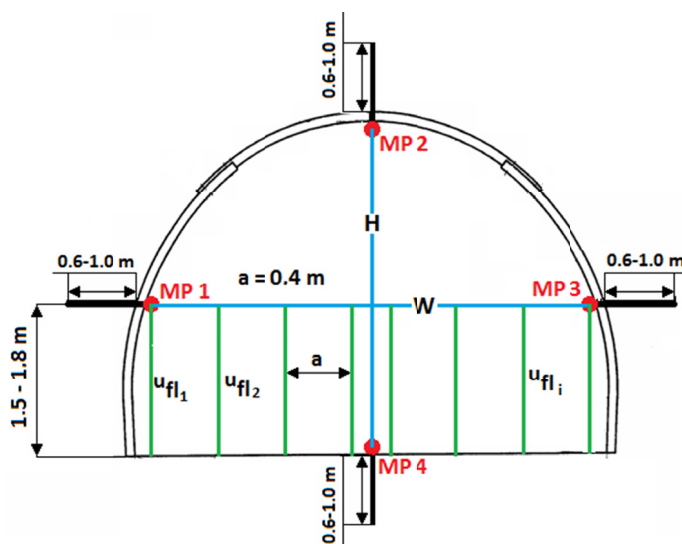

Fig. 7. Diagram of the convergence monitoring station and the distances measured

3.3. Results of convergence measurements in maingate D-2

3.3.1. Monitoring Station 735KM

In the first 420 days period, the measurements on 735KM station showed very little convergence of the opening. The recorded values of the changes were: width of gallery $\Delta W_w = 34$ cm, height $\Delta H_w = 45$ cm, and the maximum heave of the floor $u_{av} = 40$ cm. After 600 days since the formation of the gallery its height was 372 cm i.e. approx. 88% of the nominal height of the support. In June 2016 (about 570 days since formation) the width of the gallery was 95.2% of the nominal width. The increase of the deformation around station 735KM was recorded when the excavation face was at 110 m distance to the station. Significant changes of maingate D-2 dimensions were observed when the longwall face was 70 m close. The abutment pressure caused almost threefold increase of the vertical convergence i.e. 94 cm. At the same time the heave of the floor practically doubled from 40 cm to 85 cm. The dynamics of the convergence versus the distance to the longwall face is shown on the Fig. 8, and the values recorded on station 735KM are compiled in Table 3.

TABLE 3

Convergence of the gallery versus distance to the long wall face
– Station 735KM

Date	Width W_w [m]	Height H_w [m]	Distance to the longwall face L [m]	Gate convergence				
				Horizontal		Vertical		
				ΔW [m]	ΔW [%]	u_{fl} [m]	ΔH [m]	ΔH [%]
04/2015	6.40	4.00	765	0.10	1.5	0.11	0.23	5.4
06/2015	6.33	3.97	765	0.17	2.6	0.13	0.27	6.3
08/2015	6.28	3.92	635	0.22	3.4	0.16	0.31	7.3
10/2015	6.21	3.84	519	0.29	4.5	0.21	0.39	9.2
12/2015	6.18	3.81	419	0.32	4.9	0.26	0.42	9.9
01/2016	6.16	3.78	381	0.34	5.2	0.28	0.45	10.7
04/2016	6.15	3.78	223	0.35	5.4	0.31	0.45	10.7
06/2016	6.15	3.74	122	0.35	5.4	0.33	0.50	11.7
07/2016	6.09	3.72	110	0.41	6.3	0.34	0.51	12.1
08/2016	6.02	3.62	72	0.48	7.4	0.40	0.61	14.4
09/2016	5.91	3.41	27	0.59	9.1	0.54	0.82	19.4
10/2016	5.82	3.29	0	0.68	10.5	0.61	0.94	22.2

3.3.2. Monitoring Station 714KM

Convergence recorded on station 714KM, until the symptoms of approaching exploitation, was higher than on the station 735KM. It is suggested that this effect was due to presence of excavation edge of the above coal seam. The distance from the station to the edge was approx. 35 m. The record shows that the convergence, before the stage of intense deformations, was about 70 cm horizontally which is 11% of the initial width. In the same period the change in height was 15.4% (65 cm), of which 95% was the heave of the floor (62 cm). The first impact of the approaching abutment front was recorded when the distance between the station 714KM and the wall was approx. 90 m. The deformations increase when the distance reduces to approx. 50 m. The horizontal convergence of the side walls reached 102 cm, i.e. 1.5 times the value when the gate was still beyond the influence of the abutment pressure. Also, the vertical convergence increased to 115 cm. The rather small downward movement of the roof is noteworthy and it is the floor heave that contributes mostly to the vertical convergence. Table 4 shows the results of measurements on station 714KM.

3.3.3. Monitoring Station 650KM

There was minute horizontal squeezing observed on station 650KM in the period before the first signs of approaching wall exploitation. The change of horizontal dimension of the support was 6%, while 4 cm drop of the roof and u_{fl} – 82 cm heave of the floor was recorded. In this period, the vertical convergence reached 86 cm that constituted one fifth of the initial height of the gate. The decrease of cross-sectional area of the gate due to the longwall excavation started when the excavation front was approx. 110 m from the station. The decrease accelerated when the distance to the front was 80 m. The stress in the rock mass increase, induced by the approaching longwall excavation, was manifested by accelerating convergence that was measured

on station 650KM. The vertical convergence reached 29% (123 cm) of the initial dimension of the support. The floor heave increased 1.5 times to reach 117 cm, which was 94% of the vertical convergence. Whereas, twofold increase of the horizontal convergence was recorded which was 87% of the initial width.

TABLE 4

Convergence of the maingate D-2 versus distance to longwall face
– Station 714KM

Date	Width W_w [m]	Height H_w [m]	Distance to the longwall face L [m]	Gate convergence				
				Horizontal		Vertical		
				ΔW [m]	ΔW [%]	u_{fl} [m]	ΔH [m]	ΔH [%]
04/2015	6.03	3.77	786	0.47	7.2	0.30	0.46	10.9
06/2015	5.96	3.76	786	0.54	8.3	0.31	0.47	11.1
08/2015	5.96	3.69	656	0.54	8.3	0.37	0.54	12.8
10/2015	5.90	3.67	540	0.60	9.2	0.40	0.56	13.3
12/2015	5.89	3.63	440	0.61	9.4	0.43	0.60	14.2
01/2016	5.86	3.61	402	0.64	9.8	0.44	0.62	14.7
04/2016	5.82	3.60	244	0.68	10.5	0.47	0.63	14.9
06/2016	5.80	3.58	143	0.7	10.8	0.50	0.65	15.4
07/2016	5.78	3.49	131	0.72	11.1	0.53	0.74	17.5
08/2016	5.74	3.44	93	0.76	11.7	0.60	0.79	18.7
09/2016	5.61	3.20	48	0.89	13.7	0.61	1.04	24.5
10/2016	5.48	3.08	0	1.02	15.7	0.62	1.15	27.2

TABLE 5

Convergence of the maingate D-2 versus distance to longwall face
– Station 650KM

Date	Width W_w [m]	Height H_w [m]	Distance to the longwall face L [m]	Gate convergence				
				Horizontal		Vertical		
				ΔW [m]	ΔW [%]	u_{fl} [m]	ΔH [m]	ΔH [%]
04/2015	6.23	3.61	850	0.27	4.2	0.45	0.62	14.7
06/2015	6.23	3.53	850	0.27	4.2	0.49	0.71	16.7
08/2015	6.21	3.52	720	0.29	4.5	0.54	0.71	16.8
10/2015	6.19	3.47	604	0.31	4.8	0.57	0.76	18.0
12/2015	6.15	3.45	504	0.35	5.4	0.61	0.78	18.5
01/2016	6.14	3.43	466	0.36	5.5	0.63	0.80	18.9
04/2016	6.13	3.42	308	0.37	5.7	0.67	0.81	19.2
06/2016	6.11	3.40	207	0.39	6.0	0.70	0.83	19.6
07/2016	6.11	3.39	195	0.39	6.0	0.71	0.84	19.9
08/2016	6.10	3.37	157	0.40	6.2	0.73	0.86	20.4
09/2016	6.05	3.30	112	0.45	6.9	0.77	0.94	22.1
10/2016	5.99	3.22	85	0.51	7.8	0.84	1.01	23.9
04/2015	5.82	3.08	33	0.68	10.5	0.93	1.15	27.2
06/2015	5.69	3.00	0	0.81	12.5	1.04	1.23	29.1

The dynamics of the changes of the gate's dimensions versus the distance of the convergence stations to the exploitation front is shown on the Fig. 8.
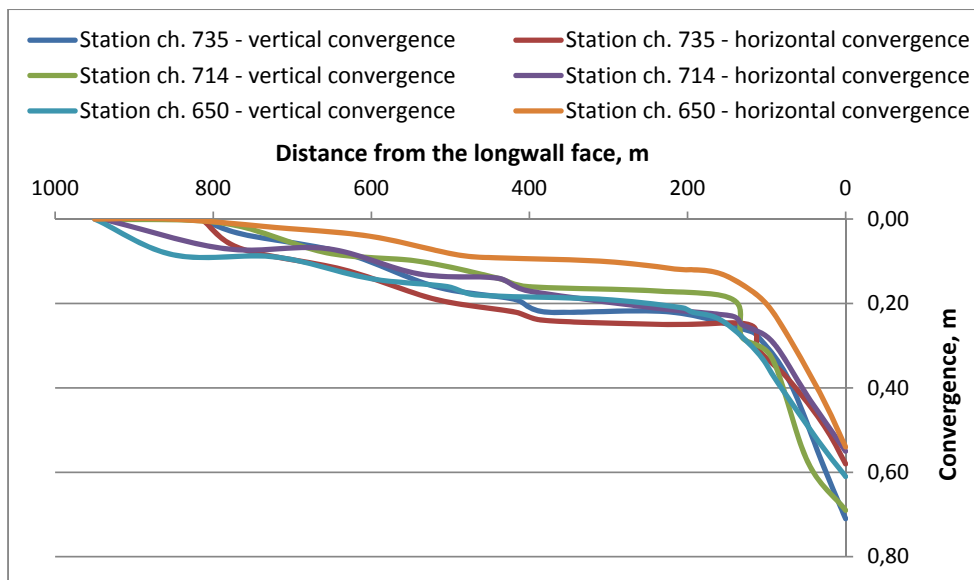

Fig. 8. Convergence of the gallery versus distance to the longwall face; monitoring period from the commencement of the excavation

In all three stations the vertical convergence was mainly due to heave of the floor (Fig. 9), while lowering of the roof ranged from several to dozen or so centimeters. The cross-sectional area of the maingate D-2 at station 735KM decreased by 6.44 m^2, i.e. approx. 28% of the initial area; at the station 714KM it decreased by 8.72 m^2, i.e. 38% of the initial value, and by 8.90 m^2 at station 630KM which was almost 40% of the initial value (Fig. 9). The average values of convergence at the longwall-maingate crossing is shown in Table 6.
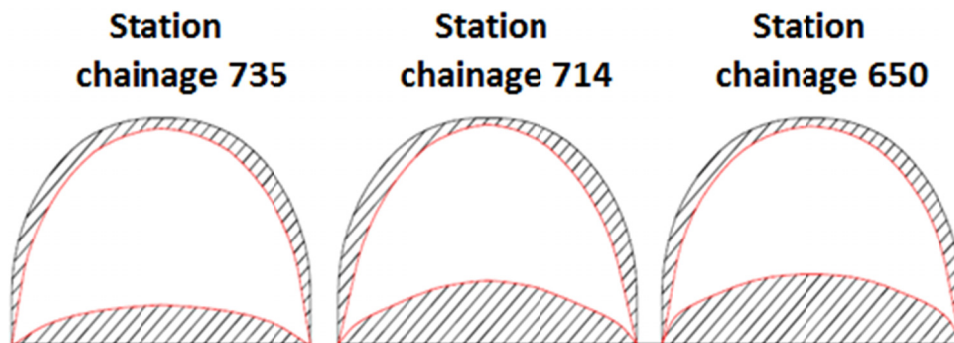
Fig. 9. Diagram of final convergence at monitoring stations

TABLE 6

Final convergence due to longwall effect recorded at monitoring stations

Convergence station	Convergence		Floor heave	Cross-sectional area of the gallery
	Horizontal	Vertical		
	[m]	[m]	[m]	[m²]
735	0.68	0.94	0.85	16.77
714	1.02	1.15	1.09	14.49
650	0.81	1.23	1.17	14.27
Average values	**0.84**	**1.11**	**1.04**	**15.18**

4. Numerical calculations

4.1. Model assumptions

Computer program Phase2, that utilizes the method of finite elements, was used to model the deformations measured in the gallery D-2. In the model, the rock mass was depicted as 2D chart consisting of ca. 12000 elements and ca. 24000 nodes (Fig. 10). Zero dislocation in horizontal and vertical direction on all boundaries of the chart was assumed as a boundary condition; taking into account initial stress related to 1000 m depth of the gallery and the average specific
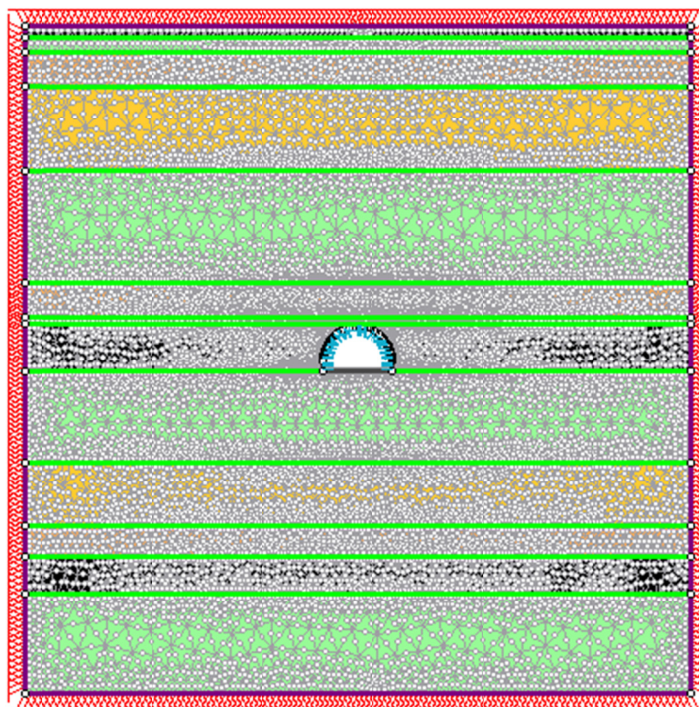
Fig. 10. The numerical model scheme

weight of the overburden. The yielding arches support ŁPCBor 12/4/V34/A, 4.225 m high, 6.5 m wide (at base), at 0.6 m spacing, and made of steel S480W (σ_y = 480 MPa and σ_u = 650 MPa) was represented in the model as a *Reinforced Concrete* with the only selected option *Reinforcement*.

The physical parameters of the rock types around the gate D-2 were obtained from laboratory tests as averaged values for all four distinguished rock types: coal, shale, sandy shale and medium grained sandstone (Tab. 7). Elasto-plastic and isotropic character of the rock mass was assumed for modeling of its behavior under the stress. The Hoek's-Brown failure criterion was selected to be used in the model. The method proposed by GIG (Prusek, 2008, 2015) was applied to evaluate post-failure parameters m_b and s of Hoek's – Brown criterion. In accordance with this method, the m_b and s parameters were gradually reduced in the course of numerical modelling until the computer-generated convergence values, also corresponding to various distance to the longwall face, were consistent with the *in-situ* measurements. Therefore, these two parameters are a function of the distance to moving excavation front.

TABLE 7

Values of rocks geomechanical parameters applied in the model

Rock type	Unit weight γ_i [kN/m^3]	UCS σ_{ci} [MPa]	Young's modulus E_i [GPa]	Poisson ratio v_i [-]
Coal	12.70	12.0	1.76	0.30
Shale	25.86	50.4	6.12	0.31
Sandy shale	25.35	53.3	8.88	0.30
Medium grained sandstone	26.08	63.3	8.26	0.27

Since the analysis of deformation and stress allows for calculation of the stress needed to for the deformation, the authors compared the normal component of stress of individual stress condition, in purpose to determine the ratio between vertical and horizontal stress that were present at the observed deformation of the gallery.

4.2. Results of the computation

4.2.1. Evaluation of rock mass quality and m_b and s parameters

For the determination the values of m_b and s parameters the appropriate RMR (Rock Mass Rating) index needs to be evaluated. These vales have to be determined for the rock mass before and during the impact of the longwall excavation. Therefore, the RMR index was obtained by both: the direct evaluation in the gallery at the stations location, and indirectly by back analysis. Comparison of these two evaluations shows very little difference, usually 1-2 score points (Tab. 8) and always the direct evaluation was higher than the inferred value. Despite that the direct evaluation is subjective, the results in Table 8 indicate that the Carboniferous rock mass is generally more fractured than it is determined by directly obtained RMR.

Figures 11-13 present charts of total displacements around convergence stations 735KM, 714KM i 630KM. It is visible that the modelled displacements increase together with closing distance to the longwall face which well compares with the in-situ measurements.

RMR index determined directly and obtained from the back analysis

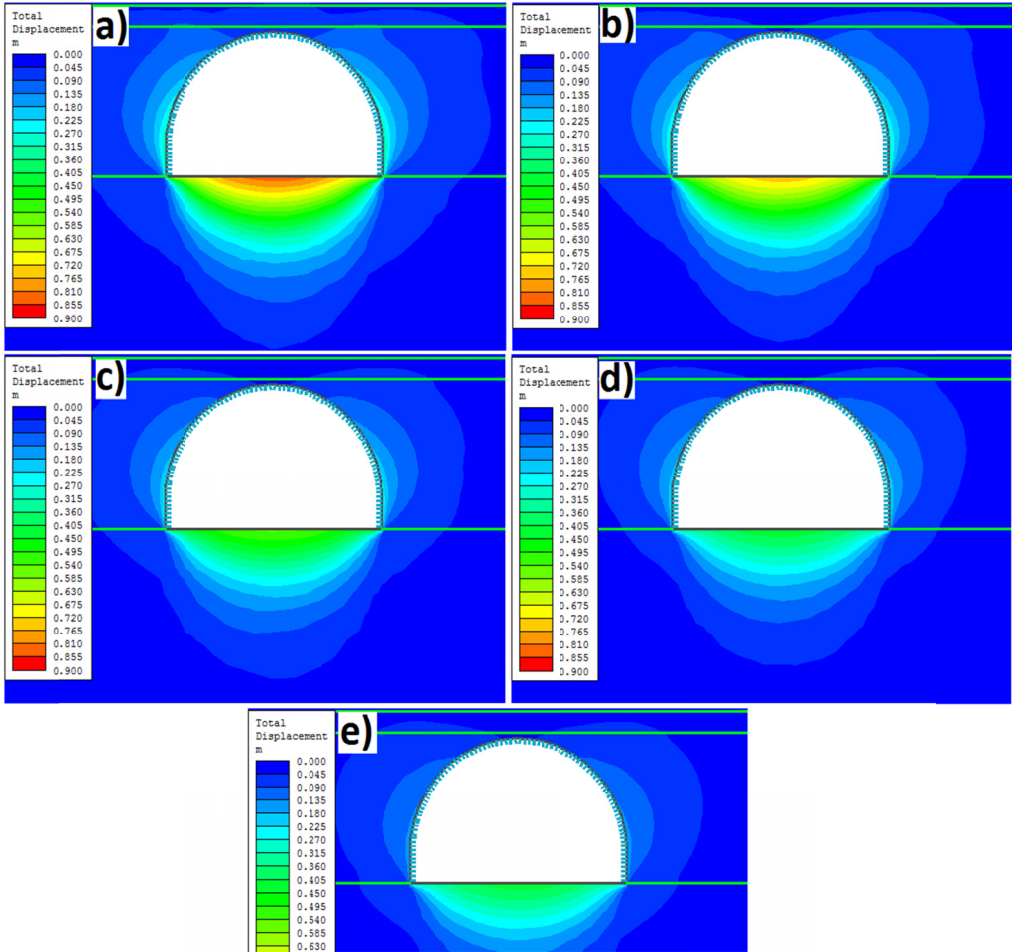| Station	RMR determined directly	RMR from reverse analysis
735	50	48
714	46	45
650	43	41

Fig. 11. Charts of the total displacement around station 735KM: a) 0 m before the longwall face,
b) 27 m before the longwall face, c) 72 m before the longwall face, d) 110 m before the longwall face,
e) 122 m before the longwall face

Through the process of adjusting the m_b and s parameters to obtain convergence values similar to *in-situ* measurements it was also possible to draw the relationship between these parameters and the distance to the longwall face for all types of rock present around the gallery, i.e. coal,
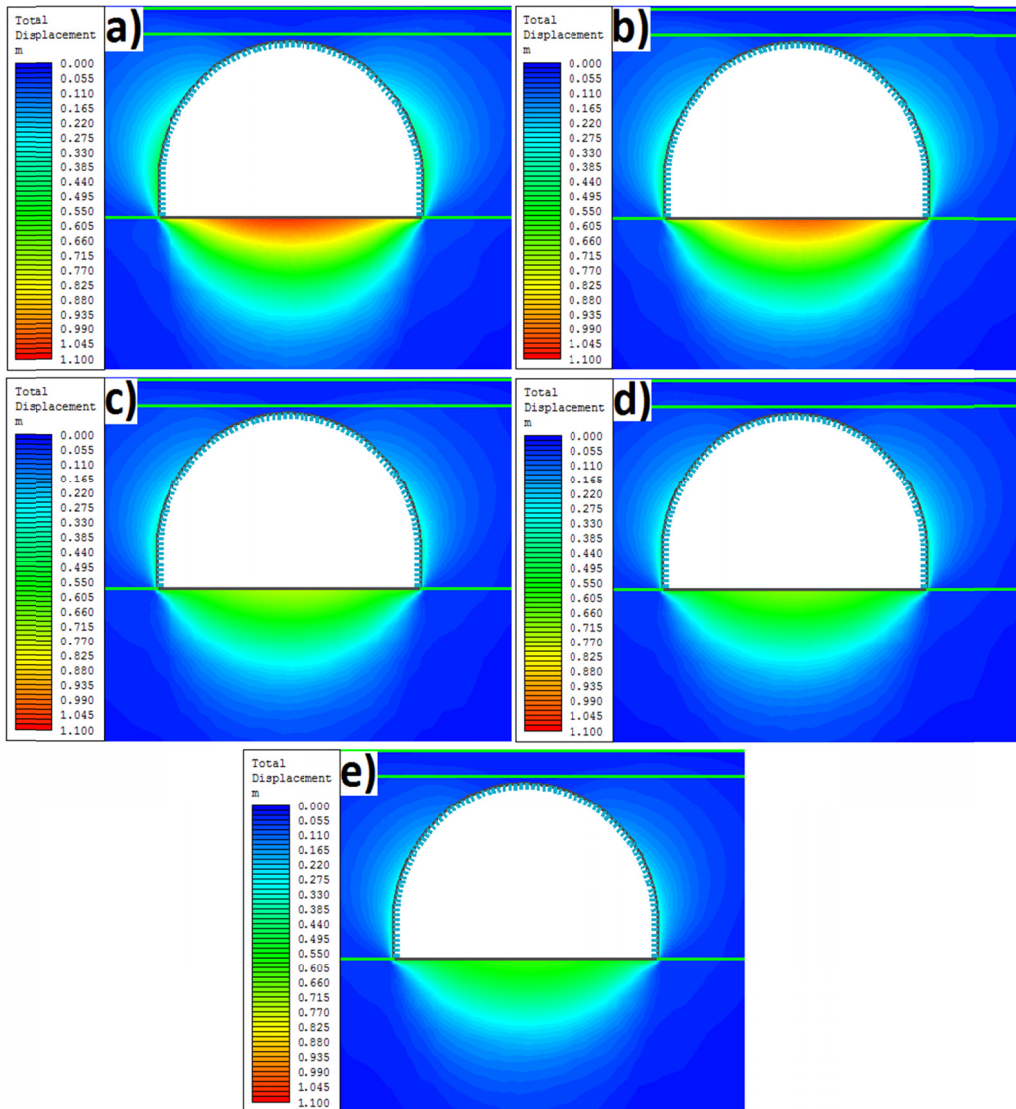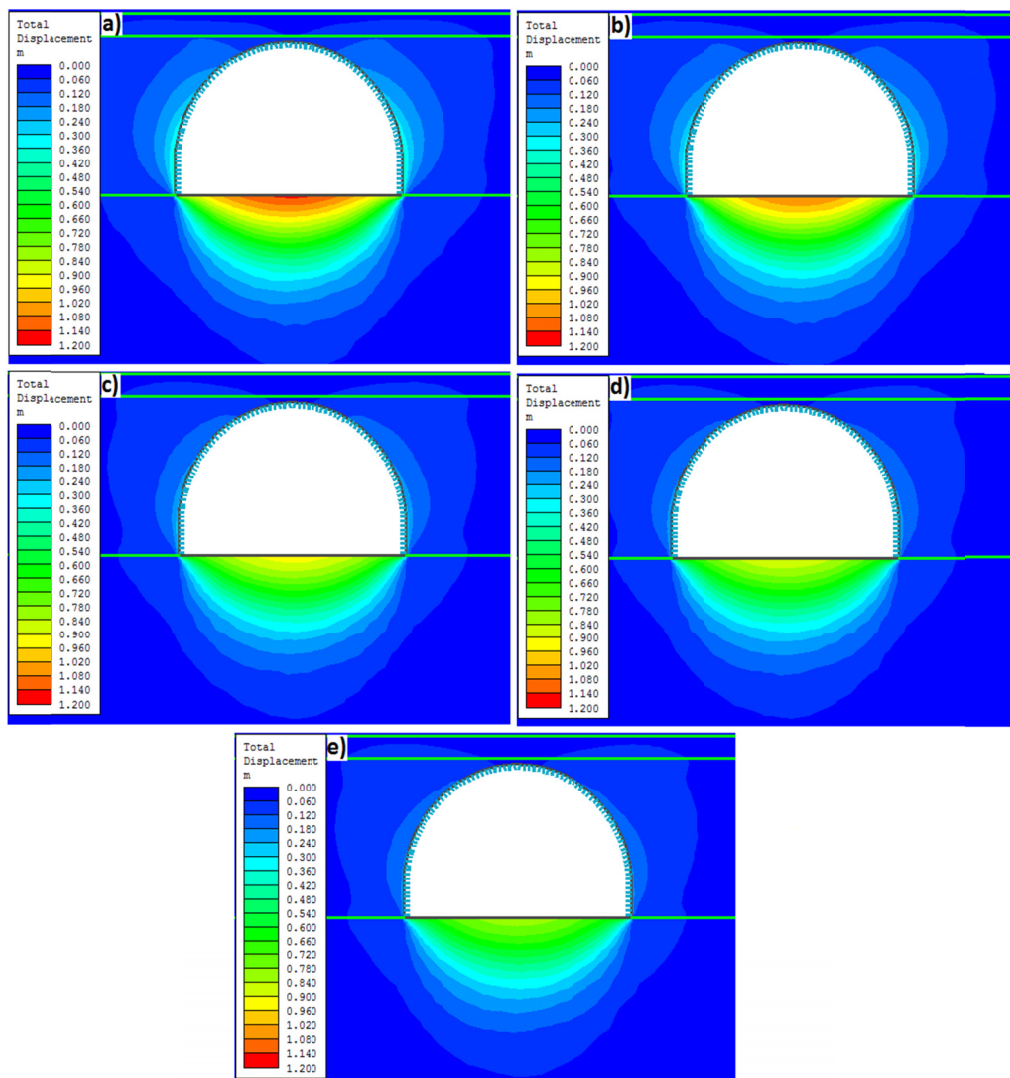
Fig. 12. Charts of the total displacement around station 714KM: a) 0 m before the longwall face,
b) 48 m before the longwall face, c) 93 m before the longwall face, d) 131 m before the longwall face,
e) 143 m before the longwall face

shale, sandy shale and medium grained sandstone (Fig. 12-17). Table 8 presents the post-failure values of m_b and s as well as the equations that could be used to calculate their change after the failure versus the distance to the longwall face. The analysis of the obtained m_b and s values shows the that the biggest drop is in case of shale and coal. The value of parameter s for coal at the crossing longwall face – main gate is 5 times lower than in the zones beyond the impact of the longwall excavation (Fig. 13, 15 and 17). Parameters m_b and s for medium grained sandstone

Fig. 13. Charts of the total displacement around station 650KM: a) 0 m before the longwall face,
b) 33 m before the longwall face, c) 85 m before the longwall face, d) 112 m before the longwall face,
e) 157 m before the longwall face

show approx. 35÷45% drop in value. The least drops of the values appear for shale and sandy shale reaching approx. 28÷33%.

It is noteworthy that the coefficient of determination R^2 for the equations cited in Table 9 is very high, and it varies from 0.7 to 0.98 for m_b parameter, and from 0.86 to 0.99 for s parameter. The correlation between the parameters and the distance to the longwall face is comparable for all investigated rock types that confirms the paramount effect of the longwall excavation on destruction of the surrounding rocks.
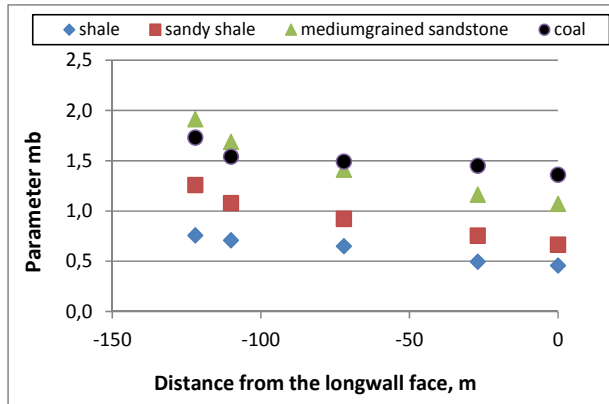
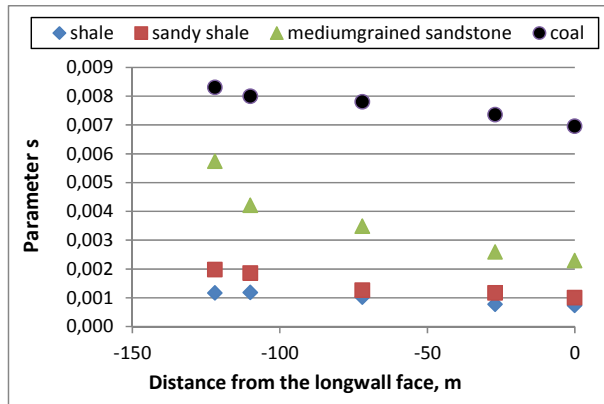Fig. 12. Change of the parameter m_b versus distance to the wall front – station 735KM

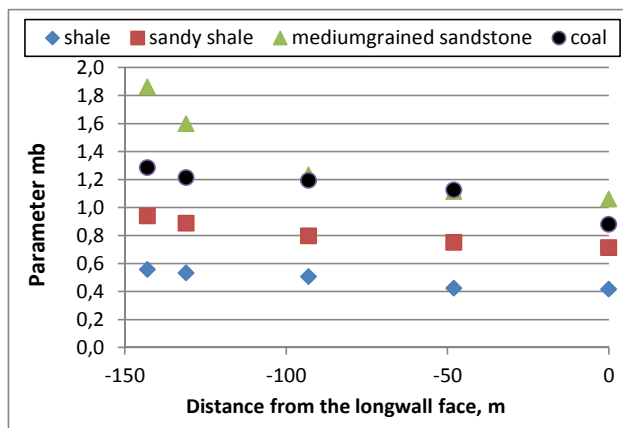Fig. 13. Change of the parameter s versus distance to the wall front – station 735KM

Fig. 14. Change of the parameter m_b versus distance to the wall front – station 714KM
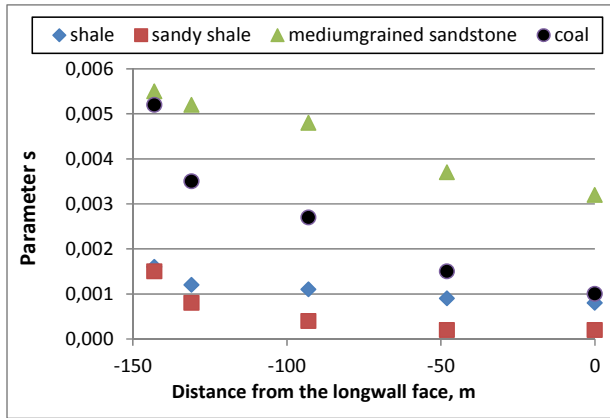
112

Fig. 15. Change of the parameter s versus distance to the wall front – station 714KM
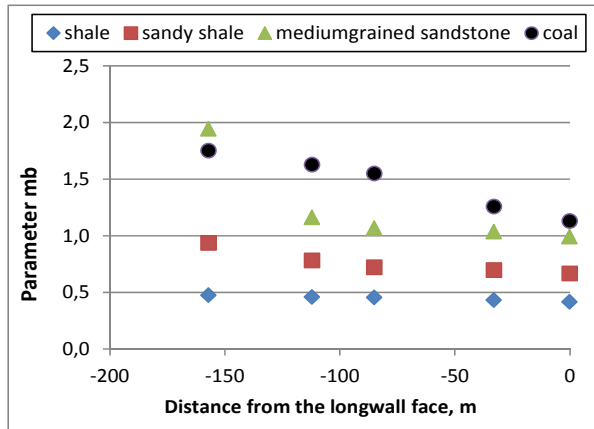

Fig. 16. Change of the parameter m_b versus distance to the wall front – station 650KM
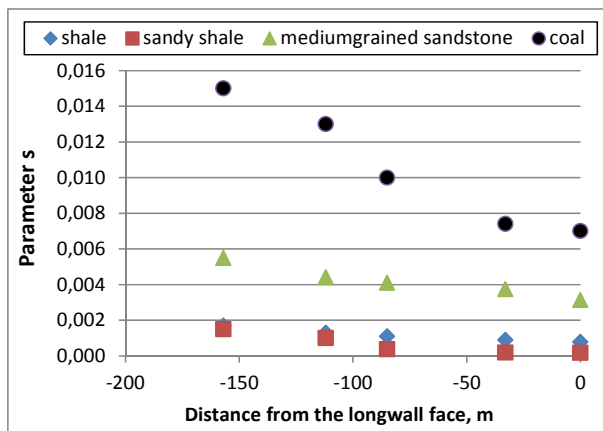

Fig. 17. Change of the parameter s versus distance to the wall front – station 650KM

The empirical rock parameters *m* and *s* of the Hoek-Brown failure criterion without the longwall effect and the regression equation representing their changes versus the distance to the longwall face

| Station | Rock type | Hoek-Brown empirical parameters | | | | | |
| | | Intact rock | | Fractured rock next to the longwall face | | | |
		m_b	s	m_{bf}	R^2	s_f	R^2
735	shale	1.327	0.0022	$m_b = 0.454e^{-0.004d}$	0.978	$s = 0.0007e^{-0.004d}$	0.974
	sandy shale	1.873	0.0031	$m_b = 0.658e^{-0.005d}$	0.984	$s = 0.0010e^{-0.005d}$	0.902
	mediumgrained sandstone	2.810	0.0060	$m_b = 1.042e^{-0.005d}$	0.980	$s = 0.0022e^{-0.007d}$	0.947
	coal	1.561	0.0080	$m_b = 1.632e^{-0.002d}$	0.818	$s = 0.0070e^{-0.001d}$	0.971
714	shale	1.192	0.0022	$m_b = 0.404e^{-0.002d}$	0.931	$s = 0.0008e^{-0.004d}$	0.886
	sandy shale	1.683	0.0031	$m_b = 0.696e^{-0.002d}$	0.937	$s = 0.0001e^{-0.014d}$	0.861
	mediumgrained sandstone	2.525	0.0060	$m_b = 0.979e^{-0.004d}$	0.855	$s = 0.0010e^{-0.011d}$	0.981
	coal	1.403	0.0080	$m_b = 0.933e^{-0.002d}$	0.860	$s = 0.0032e^{-0.004d}$	0.975
650	shale	1.033	0.0022	$m_b = 0.420e^{-0.001d}$	0.982	$s = 0.0008e^{-0.005d}$	0.988
	sandy shale	1.459	0.0031	$m_b = 0.647e^{-0.002d}$	0.869	$s = 0.0001e^{-0.015d}$	0.936
	mediumgrained sandstone	2.189	0.0060	$m_b = 0.899e^{-0.004d}$	0.701	$s = 0.0067e^{-0.005d}$	0.961
	coal	1.355	0.0080	$m_b = 1.153e^{-0.003d}$	0.965	$s = 0.0032e^{-0.003d}$	0.966

From the results in Table 9 it can be concluded that the average drop in value of the Hoek-Brown failure criterion parameters depends on the rock types building the rock mass. In case of the rock types around the main gate D-2 the regression equations are as follows:

– for shale: $m_b = 0.426e^{-0.0023d}$
$s = 0.0008e^{-0.0043d}$

– for sandy shale: $m_b = 0.667e^{-0.0030d}$
$s = 0.0004e^{-0.0113d}$

– for sandstone: $m_b = 0.974e^{-0.0043d}$
$s = 0.0033e^{-0.0077d}$

– for coal: $m_b = 1.240e^{-0.0023d}$
$s = 0.0045e^{-0.0027d}$

The obtained regressions are different than the so far published by Prusek (2008, 2015) for the Upper Silesia Coal Basin. The differences of the exponent and the constant term are up to 10%, and occasionally up to 100%. This observation proves that the diversity of properties of the Carboniferous sedimentary rocks, even within relatively small mining area, is too big for formulating universal equation to describe each rock type behavior during destruction.

4.2.2. Evaluation of the ratio between horizontal and vertical stress

Figures 18-20 present charts of principal stresses σ_1 and σ_2 at all three cross-sections of the main gate D-2. The stress condition depicted on the charts was the cause of earlier described de-

114

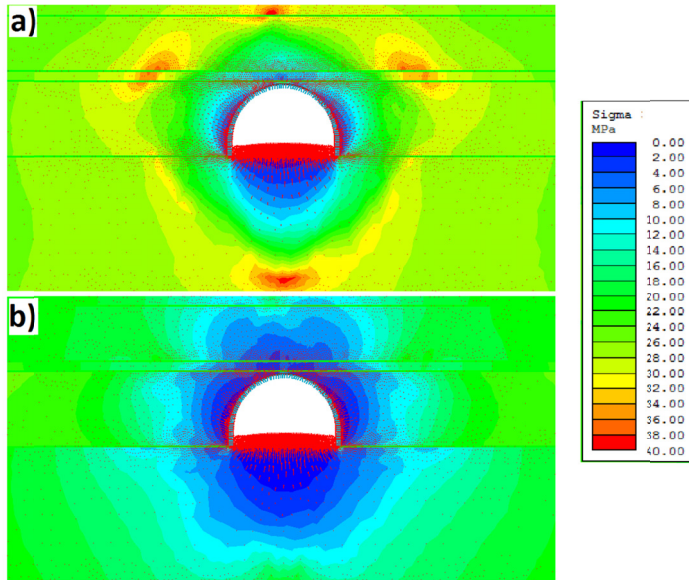

Fig. 18. Charts of the principal stresses around convergence station 745KM at the zero-distance
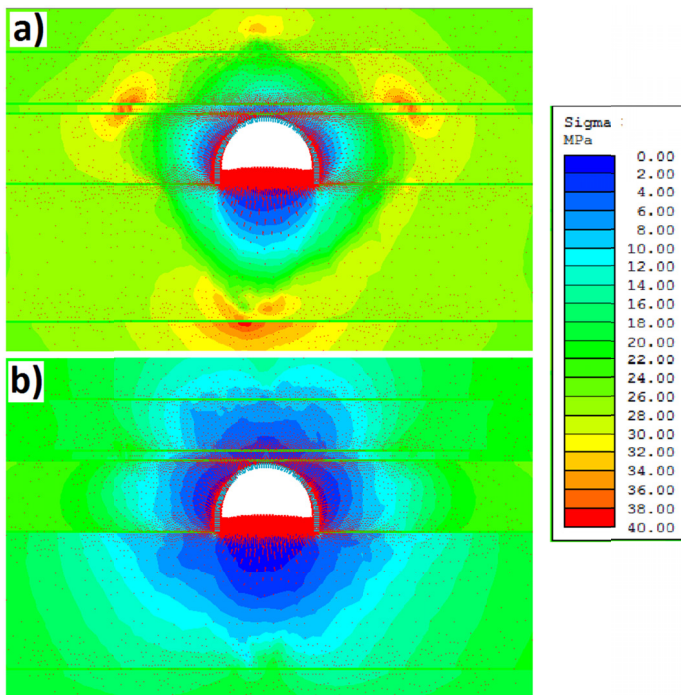to the longwall face a) principal stress σ_1, b) principal stress σ_2

Fig. 19. Charts of the principal stresses around convergence station 714KM at the zero-distance
to the longwall face a) principal stress σ_1, b) principal stress σ_2

formations of the gallery. It was assumed that the stress values in the zones beyond the contour of the gallery, at the point when failure of the rock and dissipation of stress was observed, represent the maximum stress the that the rock can bear. The analysis of the stress direction (Fig. 18-20) shows that further from the gallery the vectors assume vertical and horizontal direction, hence the principal stresses in such locations can be considered as vertical and horizontal stress. At the same time, the stress trajectories show the horizontal stresses are bigger. The differences of stress between all three stations are insignificant because the simulation took into account the different initial stress in these locations related to their different depths.

That way obtained maximum values of principal stresses (Tab. 10) show that in all three cases the horizontal stresses are greater than vertical stresses. The horizontal stresses range between

TABLE 10

The ratio of the principal stresses at the convergence stations

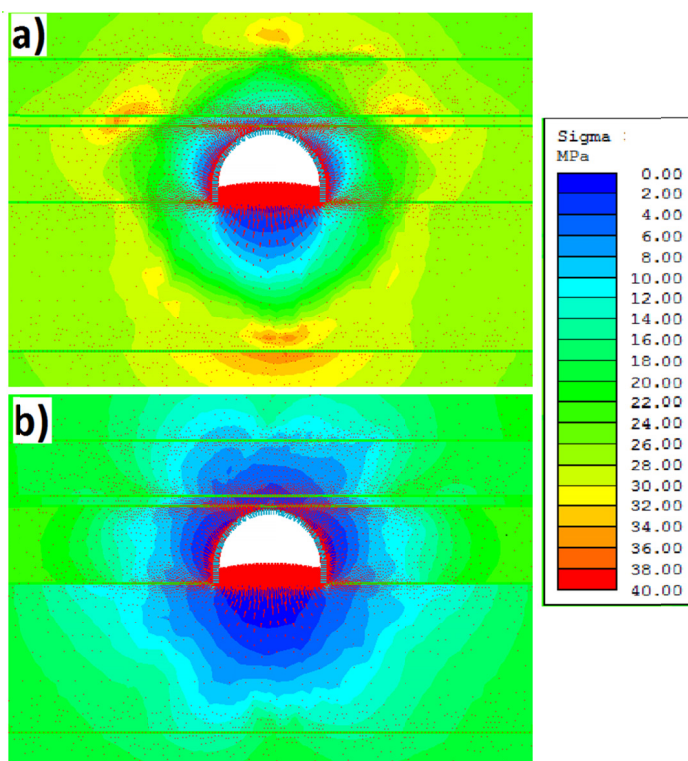| Station	$\sigma_{1max} = \sigma_x$	$\sigma_{2max} = \sigma_y$	σ_x / σ_y
735	39.85	24.68	1.61
714	37.28	24.56	1.52
650	35.50	24.46	1.45

Fig. 20. Charts of the principal stresses around convergence station 650KM at the zero-distance to the longwall face a) principal stress σ_1, b) principal stress σ_2

35.5 MPa and 39.8 MPa, while the vertical between 24.5 MPa to 24.7 MPa. Therefore, the ratio horizontal to vertical stress remains in 1.4-1.6 range, hence for the measured deformations in the D-2 gate the horizontal stress had to be approx. 1.5 times biger than the vertical stress. The performed analysis confirmed the observations in the mining galleries of JSW (Jastrzębie Coal Company) where common are undercutting of arch legs, inward buckling of the sidewalls, and downward bending of crown arch.

5. Summary and discussion

The effect of progressing longwall excavation on the process of destruction of the rocks in its vicinity is significant. Fracturing of the rock causes a change of stress conditions in the rock mass which in consequence leads to convergence of the gateroads. The destruction of rock intensifies together with the approaching excavation front. The development of fractures together with the decreasing distance to the longwall face cause the change of the parameters of the failure criterion as the rock mass is not able to withstand the increasing stress. Therefore, the assumption of the same geomechanical properties of rocks within and beyond the longwall impact zone is incorrect.

The Hoek's-Brown hypothesis implies that the empirical parameters m_b and s for each rock type change continuously with the approaching excavation front. Despite the continuous character of this change it is difficult to provide *ad hoc* the true values of these parameters However, it is feasible based on *in-situ* investigation and convergence measurements. This approach allows for determination at what distance the longwall excavation starts affecting the stress condition and deformation of the rock mass, and for determination of empirical parameters m_b and s of Hoek-Brown criterion from the measured convergence. The numerical analysis carried out by the authors shows that the change of these parameters versus distance d to the longwall face can be described by exponential equation:

$$P = a \cdot e^{-b \cdot d} \tag{5}$$

where: P is the parameter of Hoek-Brown hypothesis, while a and b are the constants of the equation.

The obtained functions representing the change of m_b and s parameters for shale, sandy shale, coal and medium grained sandstone are significantly different from the earlier works by Central Mining Institute (Prusek, 2008; 2015) as to the value of exponent and constant term. This observation proves that the diversity of properties of the Carboniferous sedimentary rocks, even within relatively small mining area, is too big for formulating universal equation to describe each rock type behavior during destruction. The research and development of this kind of equation should be limited to individual lithotypes (based on earlier mineralogical investigation), or limited to one exploitation field. From practical point of view, a research carried out in the first of the designed gateroads should be sufficient for reliable evaluation of the parameters characterizing the failure properties of rocks. This evaluation should be valid for all other galleries if assuming relatively uniform geological conditions all over the mining field.

In the case of maingate D-2, and based on *in-situ* measurements it was found that the rock mass deformations started at approx. 100 m from the longwall face, and intensified at the distance

of approx. 40-60 m. The recorded convergence at longwall-maingate crossing reached values 1.5-3 times higher than at the same stations yet far from the longwall face. From the gallery stability point of view these magnitudes are particularly high, and could not be obtained from numerical modeling without lowering the geomechanical properties of the rock mass.

Noteworthy are also the values of horizontal stress generated from the numerical analysis, which are 1.5 times greater than the corresponding values of vertical stress. Such a high horizontal stress significantly contributes to the rock mass deformation process, especially causing the heave of unsupported floor of the gateroad.

References

Basarir H., Oge I.F., Aydin O., 2015. *Prediction of the stresses around main and tailgates during top coal caving by 3D numerical analysis*. International Journal of Rock Mechanics & Mining Sciences **76**, 88-97.

Bieniawski Z.T., 1987. *Strata control in mineral engineering*. Balkema, Rotterdam.

Brady B., Brown E., 2006. *Rock mechanics for underground mining*. Springer, The Netherlands.

Brown E.T., Hoek E., 1978. *Trends in Relationships between Measured In-Situ Stresses and Depth*. Int. J. Rock Mech. Min. Sci. & Geomech. Abstr. **15**, 211-215.

Butra J., Dębkowski R., Laskowicki S., Pawelus D., 2013. *Określenie parametrów pola naprężeń w kopalni Rudna na podstawie badań in-situ*. Proceedings of: XXII Szkoła Eksploatacji Podziemnej, 18-22 lutego 2013 Kraków, 1-12 (in Polish).

Chudek M., Duży S., 2002. *Deformacje korytarzowych wyrobisk przygotowawczych drążonych w strefach wpływu czynnego frontu eksploatacyjnego w świetle pomiarów dołowych*. Zeszyty Naukowe Politechniki Śląskiej, Seria Górnictwo **254**, 265-273 (in Polish).

Faria Santos C. & Bieniawski Z.T., 1989. *Floor Design in Underground Coal Mines*. Rock Mechanics and Rock Engineering **22**, 249-271.

Han J., Zhang P.T., 2010. *The in situ stress state of Kailuan mining area*. 5th International Symposium ISRM "In situ rock stress", Beijing.

Handley M.F., 2013. *Pre-mining stress model for subsurface excavations in southern Africa*. The Journal of The Southern African Institute of Mining and Metallurgy **113**, 449-471.

Herezy Ł., 2013. *Prognozowanie zasięgu wzmożonych deformacji chodnika przyścianowego na podstawie monitoringu pracy obudowy zmechanizowanej w warunkach kopalni LW Bogdanka SA*. Doctor thesis (unpublished – in Polish).

Hoek E., 2016. *Practical Rock Engineering*. Chapter 12: Rock Mass Properties, 2016 (on-line).

Hosseini N., Goshtasbi K., Oraee-Mirzamani B., Gholinejad M., 2014. *Calculation of periodic roof weighting interval in longwall mining using finite element method*. Arabian Journal of Geoscience **7**, 1951-1956, DOI 10.1007/s12517-013-0859-8.

Islam Md.R. Hayashi D., Kamruzzaman A.B.M., 2009. *Finite element modeling of stress distributions and problems for multi-slice longwall mining in Bangladesh, with special reference to the Barapukuria coal mine*. International Journal of Coal Geology **78**, 91-109.

Junker M., Achilles P., 2006. *Gebirgsbeherrschung von Flözstrecken*. Verlag Glückauf, Essen.

Lian-guo W., Yu W., Jian S., 2009. *Three-dimensional numerical simulation on deformation and failure of deep stope floor*. Procedia Earth and Planetary Science **1**, 577-584.

Lubosik Z., Walentek A., 2016. *Przejawy ciśnienia eksploatacyjnego w chodnikach przyścianowych zlokalizowanych na głębokości około 1000 m – badania dołowe*. Przegląd Górniczy **3**, 8-16 (in Polish).

Majdi A., Hassani F.P., 1989. *Access tunnel convergence prediction in longwall coal mining*. International Journal of Mining and Geological Engineering **7**, 283-300.

Majdi A., Hassani F.P., Yousef Nasiri M., 2012. *Prediction of the height of destressed zone above the mined panel roof in longwall mining*. International Journal of Coal Geology **98**, 62-72.

Majcherczyk T., Małkowski P., 2003. *Wpływ frontu ściany na wielkość strefy spękań wokół wyrobiska przyścianowego*. Wiadomości Górnicze **1**, 20-29 (in Polish).

Makówka J., 2015. *Method of determining the triaxial stress state in the rock mass with directed hydrofracturing*. Arch. Min. Sci. **60**, 3, 729-741.

Małkowski P., Niedbalski Z., Majcherczyk T., 2016a. *Investigations of hard coal mine roadways stability in stratified rock*. Conference: Proceedings of: Ground Support 2016, E. Nordlund, T.H. Jones and A. Eitzenberger (eds), Lulea, Sweden.

Małkowski P., Niedbalski Z., Majcherczyk T., 2016b. *Roadway design efficiency indices for hard coal mines*. Acta Geodyn. Geomater. **13**, 2(182), 201-211. DOI: 10.13168/AGG.2016.0002.

Mark C., 1991. *Horizontal stress and its effects on longwall ground control*. Mining Engineering. November 1991, 1356-1360.

Mohammadi S., Ataei M., Kakaie R., 2018. *Assessment of the Importance of Parameters Affecting Roof Strata Cavability in Mechanized Longwall Mining*. Geotech. Geol. Eng., https://doi.org/10.1007/s10706-018-0490-2.

Nemcik J.A., Gale W., Fabjanczyk M., 2006. *Methods of interpreting ground stress based on underground stress measurements and numerical modelling*. In Proceedings of 7th Underground Coal Operators Conference (N. Aziz and W. Keilich eds.), University of Wollongong, NSW, Australia, 104-112.

Niełacny P., 2009. *Dobór technologii utrzymania wyrobisk przyścianowych w jednostronnym otoczeniu zrobów na podstawie pomiarów przemieszczeń górotworu*. Rozprawa doktorska (materiały niepublikowane)

Niedbalski Z., Małkowski P., Majcherczyk T., 2013. *Monitoring of stand-and-roof-bolting support: design optimization*. Acta Geodyn. Geomater. **10**, 2 (170), 215-226, DOI: 10.13168/AGG.2013.0022.

Peng S., 2006. *Longwall Mining 2nd Edition*. West Virginia University Press, Morgantown.

Prusek S., 2008. *Metody prognozowania deformacji chodników przyścianowych w strefach wpływu eksploatacji z zawałem stropu*. Prace Naukowe Głównego Instytutu Górnictwa, nr 874, Katowice (in Polish).

Prusek S., 2015. *Changes in cross-sectional area of gateroads in longwalls with roof caving, ventilated with "U" and "Y" systems*. Archives Of Mining Sciences **60**, 2, 549-564.

Sabanimashcool M., & Li C.C., 2012. *Numerical modelling of longwall mining and stability analysis of the gates in the coal mine*. International Journal of Rock Mechanics & Mining Sciences **51**, 24-34.

Singh G.S.P., 2015. *Conventional approaches for assessment of caving behavior and support requirement with regard to strata control experiences in longwall workings*. Journal of Rock Mechanics and Geotechnical Engineering **7**, 291-297.

Staš L., Knejzlik J., Palla L., Souček K., Waclawik P., 2011. *Measurement of Stress Changes Using a Compact Conical-ended Borehole Monitoring*. Geotechnical Testing Journal **34**, 6, November 2011, 685-693, DOI: 10.1520/GTJ102794.

Torano J., Rodrıguez Dıez R., Rivas Cid J.M., Casal Barciella M.M., 2002. *FEM modelling of roadway driven in fractured rock mass longwall influence*. Computers and Geotechnics **29**, 411-431.

Ulusay R., Hudson J.A. (eds.), 2007. *The complete ISRM suggested methods from rock characterization, testing and monitoring: 1997-2006*. ISRM Turkish National Group, Ankara.

Technical documentation of D-2 Maingate, 2016. „Borynia-Zofiówka-Jastrzębie" Hard Coal Mine (unpublished – in Polish).

Waclawik P., Kukutsch R., Konicek P., Ptacek J., Kajzar V., Nemcik J., Staš L., Souček K., Vavro M., 2017. *Stress State Monitoring in the Surroundings of the Roadway Ahead of Longwall Mining*. Procedia Engineering **191**, 560-567, DOI: 10.1016/j.proeng.2017.05.218.

Wardas A., Bobek R., Śledź T., Mąka B., Ratajczak A., 2013. *Utrzymanie chodnika przyścianowego 20A w pokładzie 405/3 w warunkach zagrożeń naturalnych kopalni „Knurów-Szczygłowice" Ruch Knurów*. Górnictwo i Geologia **8**, 1, Wydawnictwo Politechniki Śląskiej, 125-139 (in Polish).

Wrana A., Prusek S., 2016. *Ocena spękań filarów węglowych pozostawianych pomiędzy chodnikami przyścianowymi*. Przegląd Górniczy **3**, 17-27 (in Polish).

Yasitli N.E., Unver B., 2005. *3D numerical modeling of longwall mining with top-coal caving*. International Journal of Rock Mechanics & Mining Sciences **42**, 219-235.